3D PRINTING AND ADDITIVE MANUFACTURING
Volume 3, Number 4, 2016

DOI: 10.1089/3dp.2016.0036

ORIGINAL ARTICLE

Three-Dimensional-Printed Carnivorous Plant with Snap Trap

Mikail Temirel,[1,*] Bekir Yenilmez,[2,*] Stephanie Knowlton,[1,*] Jason Walker,[2] Ashwini Joshi,[1] and Savas Tasoglu[1,2]

Abstract

Three-dimensional (3D) printing has a variety of applications, from efficient iterations of engineering designs to fabrication of tissues for regenerative medicine. In soft robotics, 3D-printed functional materials can be used to mimic biological functions. Soft robotics overcomes some of the limitations of traditional rigid-body robotics through the ability to conform to different shapes and to be pneumatically controlled. Although soft robotics has been studied extensively by curing elastomers, 3D printing of flexible soft robotic components remains a challenge. Thus, we propose a method to easily fabricate a soft robotic device by using a stereolithography-based 3D printer and a flexible resin. Here, we have designed a device with a soft material composition, a pneumatic control device, and an integrated touch-based sensor to actuate a grasping motion in response to an object coming in close proximity to the sensor, mimicking the natural motion of a carnivorous plant. Characterization of the geometric and kinematic features of the plant leaves shows the dependence of the plant leaves' opening and closing motion on the touch signal provided. In the future, such soft hybrid robotic structures can be useful for biosensing, smart clothes, prosthetic designs, and other soft robotics applications.

Keywords: 3D printing, biosensor, soft robotics, grasping, venus flytrap

Introduction

THE FUTURE OF remobilizing disabled patients may lie in soft robotics. According to the U.S. Census Bureau, in 2010, 56.7 million people (19% of the population) had a disability.[1] Although disability is defined broadly, a significant portion of these disabilities are motor disabilities, which limit a person's ability to perform daily tasks. It is estimated that about 19.9 million people have difficulty lifting or grasping.[1] Soft robotics may be helpful to such patients to complete these tasks, including handling delicate objects.[2] Although conventional rigid-body robotic devices are generally constructed from metal structures with a limited range of motion, soft robotics does not use a rigid skeleton for mechanical strength.[3] Soft robotics, thus, may replace traditional robotic grippers in environments where rigid grippers cannot be used, expanding both the capability to fabricate functional prosthetics and to carry out food handling and certain industrial applications.[4] Soft robotics has also been used to replicate the movement of animals like the octopus[5] and plants like *Salvinia molesta.*[6,7]

Additive manufacturing is a versatile and broadly applicable technology that has experienced significant technological advancements in the recent years.[8,9] With several printing approaches now commercially available in desktop-style printers, three-dimensional (3D) printing is easily accessible to consumers and scientists alike and may be applied to efficiently and simply design and optimize a variety of devices.[10–14] In addition, with the rapidly expanding range of the printable materials available offering a broad selection of mechanical properties, such as flexible materials, the field of possibilities is even further expanded into applications such as soft robotics.

Although 3D printing of soft materials has been previously implemented for prosthetics, such as an ear prosthesis,[15] the approach presented here involves pneumatic control of the deformable soft robotic structure in response to an external stimulus. The design proposed is nature inspired, mimicking

Departments of [1]Biomedical Engineering and [2]Mechanical Engineering, University of Connecticut, Storrs, Connecticut.
*These three authors contributed equally to this work.

Opposite page: 3D printed carnivorous plant. This flower mimics the natural motion of a carnivorous plant. The soft material composition of the flower was printed in two parts using a stereolithography-based 3D printer and flexible resin. *Photo credit:* Mikail Temirel.

the motion of a carnivorous plant. The *Dionaea muscipula*, commonly known as the Venus flytrap, is the fastest moving organism in the plant kingdom with the ability to snap its jaw-like leaves closed within 100 ms.[16] The exact mechanism that rapidly closes the leaves is not fully understood; leading theories include cell wall loosening activated by acidification, elastic deformation due to instability, or fast-opening water channels.[17] It has also been demonstrated that an electrical current can stimulate the reaction,[18] but further research is needed to define this action of the *Dionaea muscipula*. The plant's sensor detects when a fly or another object comes into contact with the fine hairs located inside the ''mouth'' of the plant, sending a signal to close the snap and begin digestion of the insect. This action of the *D. muscipula* can be useful to the fields of biomedical and mechanical engineering. The design presented here mimics the closing actions of a Venus flytrap, and it is mechanically and electrically based rather than biologically and chemically based. This design translates the naturally occurring action of the Venus flytrap to the mechanical action of a 3D-printed object. This biomimicry process provides a useful model for creating soft robotic devices.

To mimic the Venus flytrap, a small plant-like model is rapidly 3D printed by using two different types of resin (soft and rigid) on a stereolithography-based 3D printer. The design comprises a flexible material to fabricate a nature-inspired soft body device, in addition to sensors, circuitry, and pneumatic controllers to actuate mechanical movement. The shape of the leaves can be changed pneumatically by varying the air pressure in the soft, hollow part, causing an opening and closing motion that mimics the movement of the Venus flytrap. The leaf opening was characterized by the displacement of the leaves as air is pumped into the 3D-printed plant. When pressure is released, the plant closes. A touch sensor connected to an Arduino is also implemented to actuate the air supply in response to touch, creating a stimulus-responsive soft robotic device.

Methods

A Venus trap was custom designed and 3D printed based on the ''Blossom'' blooming 3D-printed flower.[19] The leaves of the flower and base were designed in SolidWorks and printed on a Titan 1 (Kudo3D, Inc., Pleasanton, CA) 3D Printer with a flexible resin (SPOT-E; Kudo3D, Inc.). When sufficient air pressure was applied within the leaf structure, the air filled the hollow spaces between the two layers of leaves, expanding the inner layer and causing the curved structure to extend. Since the flexible material underwent an elastic deformation, on releasing the air pressure the design returned to its original shape, closing the leaves toward one another, as shown in Figure 1b. The computer-aided design (CAD) model cross-sections are shown in Figure 2a–d to demonstrate the two-layer leaf design. The inner leaves assisted expansion by pushing the outer leaves outward, whereas the outer leaves acted as a mechanical support.

To integrate the pneumatic control to set the flower to its ''open'' state, the air spaces inside the assembled flower were connected to an air pump (Paradox Robotics, New York, NY) through elastic vinyl tubing (OD = 1/4″) and valves (Paradox Robotics). The maximum pressure was set manually by using a potentiometer connected to an Arduino input. To open the leaves, the Arduino sent a signal to open the valve and to maintain the air pressure at the set point. To maintain the air pressure, a feedback loop was initiated wherein the Arduino

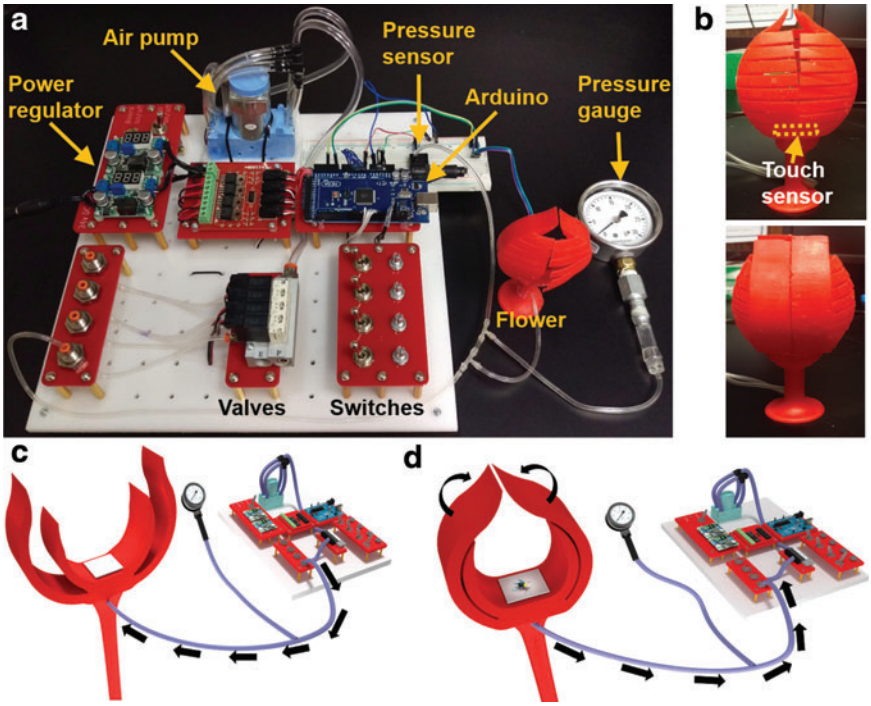

FIG. 1. Overview of the 3D-printed carnivorous plant design. **(a)** Setup with the flower, control unit, pump, pressure gauge, sensor, valve, and switches. **(b)** 3D-printed leaves of the flower (printed with a flexible resin) attached to a base (printed with rigid resin). **(c)** Schematic of setup when the flower is open, with air being pumped into the flower. **(d)** Schematic view of the closed flower when the touch sensor detects a fly, air is no longer pumped into the flower, and the air inside the flower is released with the valve. 3D, three-dimensional. Color images available online at www.liebertpub.com/3dp

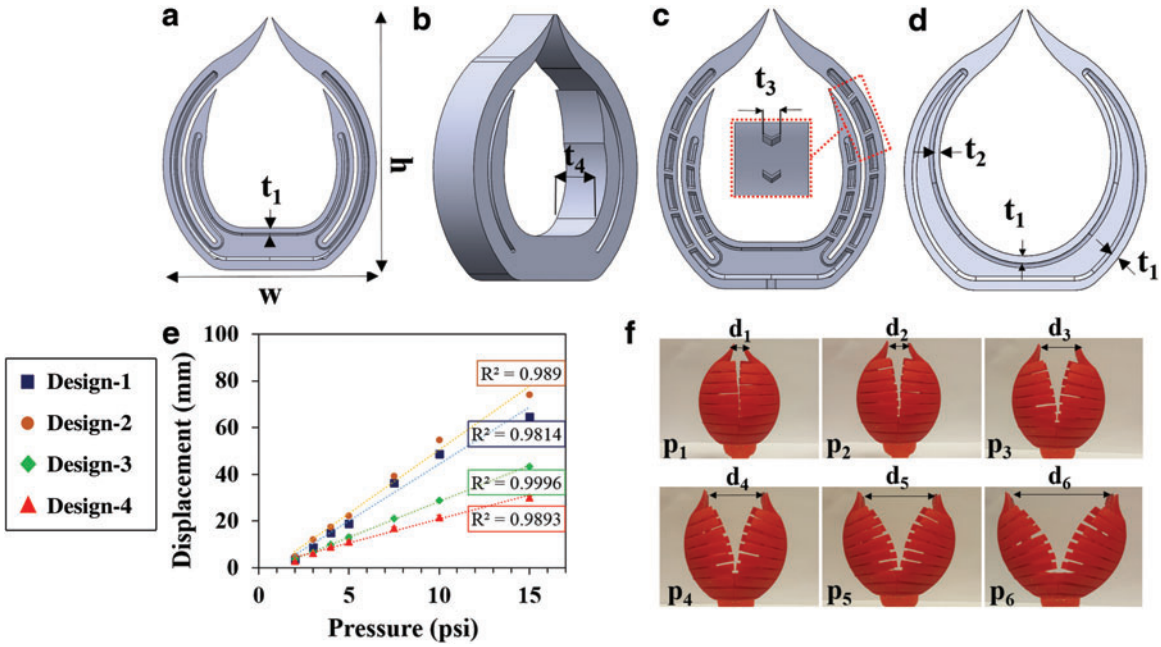

FIG. 2. Computer-aided design (CAD) views of designs and motion of the flowers under different air pressures. **(a)** Cross-sectional view of Design-1. **(b)** Design-2, 10% larger than Design-1 in all dimensions. **(c)** Design-3, a variation of Design-1 with inner supports. **(d)** Design-4, a variation of Design-1 without the inner leaves. **(e)** Displacement versus applied pressure for the four designs at seven different pressure values. **(f)** Images of Design-2 when different pressures are applied. Fifteen pounds per square inch is the maximum pressure that may be applied before the flower breaks. Color images available online at www.liebertpub.com/3dp

sensed the air pressure within the leaves via the sensor and emitted a signal to the valve (via pulse width modulation) to open, thus pumping air into the leaves while the pressure was below the set point. The system signaled the valve to close once the set point was reached and if the pressure fell below the set point, the valve was reopened until the pressure reached the set point once again. An analog pressure gauge was connected to manually validate the pressure sensor readings in parallel.

An Arduino microcontroller was integrated as a user-friendly communication platform between a touch sensor and the air pump. A capacitive touch sensor (Paradox Robotics) was mounted to the inside of the flower to sense when an object was in the vicinity of the plant and, through the Arduino-based code, caused the leaves to close by closing the valve, releasing the air pressure inside the leaves. The sensor was sensitive to both organic and inorganic materials; in these experiments, a piece of apple was lowered into the flower in the open state to trigger the closing motion. The plant remained in the closed position for a programmed period of time, defined as delay time, before reopening the valve to return to the open position. All components were mounted to laser-cut supports on the control board (Fig. 1a). A schematic view of the setup is shown in Figure 1c when the flower is open and air is pumped into the flower, separating the leaves. Figure 1d, on the other hand, shows a schematic of the closed flower after the touch sensor detects an object inside the flower, causing the valve to close and the air pressure inside the leaves to be released.

Four different leaf shapes were designed and fabricated (Fig. 2a–d). *Design-1* is the base design (63.9 mm wide by 76.2 mm in length); *Design-2* is scaled up by 10% compared with *Design-1*. *Design-3* is a modified form of *Design-1* to include inner supports that are intended to prevent the swelling of leaves under high air pressures. *Design-4* was modified to exclude the inner layer in the interest of avoiding failures at the junction at high pressure (above 15 psi). Dimensions of all designs are demonstrated in Table 1. Each design was characterized in terms of the displacement (defined as the distance between the tips of the leaves) and the opening and closing time at various pressures.

To observe leaf opening, the leaf opening motion was recorded by using a video camera, where the signal to open the plant was sent at time 0 and a pressure set point of 10 psi was applied. To observe leaf closing, the displacement over time was recorded where a pressure of 10 psi was maintained before time 0 and the signal was sent to close the plant at time 0. The displacement was measured by a caliper as the distance between the two leaf tips. The opening and closing motions of the flower were further analyzed to determine the time between the closed position and the maximum open displacement and

Table 1. Dimensions of Four Flower Designs

	Width, w (mm)	*High, h (mm)*	*Thickness, t_1 (mm)*	*Thickness, t_2 (mm)*	*Thickness, t_3 (mm)*	*Thickness, t_4 (mm)*
Design-1	63.9	76.20	2.0	2.0	N/A	15.0
Design-2	70.3	83.82	2.1	2.1	N/A	16.5
Design-3	63.9	76.20	2.0	2.0	3.0	15.0
Design-4	63.9	76.20	2.0	1.5	N/A	15.0

N/A, not applicable.

between the open position and closed position as the point at which the change in displacement reached a plateau. In the recorded video, both the position of maximum displacement while open and the closed position at which displacement reaches a plateau are apparent both visibly and through the caliper measurements. All experiments were repeated for various pressure values at least six times to demonstrate the dependence on applied pressure and the repeatability. The delay between triggering the capacitive touch sensor and the reopening of the trap was also characterized at 3, 10, 15, and 20 s.

Results and Discussion

Characterization of flowers

Using the pneumatic control system, varying air pressures were applied to each of the four flower designs in increments of 2.5 psi. The displacement, defined as the maximum separation distance between the upper tip of one leaf of the flower and the other, is shown in Figure 2e. Representative images for *Design-2* are shown in Figure 2f to demonstrate the motion. Based on these results, upon applying air pressure, the flower begins to open at very low pressures (around 2 psi). The displacement increases linearly ($R^2 > 0.9814$) with the increasing pressure up to 15 psi, which was the maximum applied pressure before the material began to rupture. At high pressures, a slight deviation from linearity is observed as the maximum displacement is reached.

Figure 2e indicates that *Design-2*, which is 10% larger than *Design-1*, has a 10% greater maximum displacement value (at 15 psi) and a 10% greater slope. Although *Design-1* and *Design-3* have the same size by all dimensions and the same thickness, the displacement of *Design-3* is lower than that of *Design-1* by about 33% due to the presence of the internal supports, which were designed to prevent swelling of the surfaces at high pressures. However, the supports also decrease the elasticity of the structure and inhibit the movement of the leaves. Lastly, *Design-4* lacks the inner leaves and was designed with a circular base and thicker walls compared with *Design-1* to prevent leaves from breaking at the junctions between the base and leaves. This modified design demonstrated the lowest displacement values, showing a 50% reduction in the

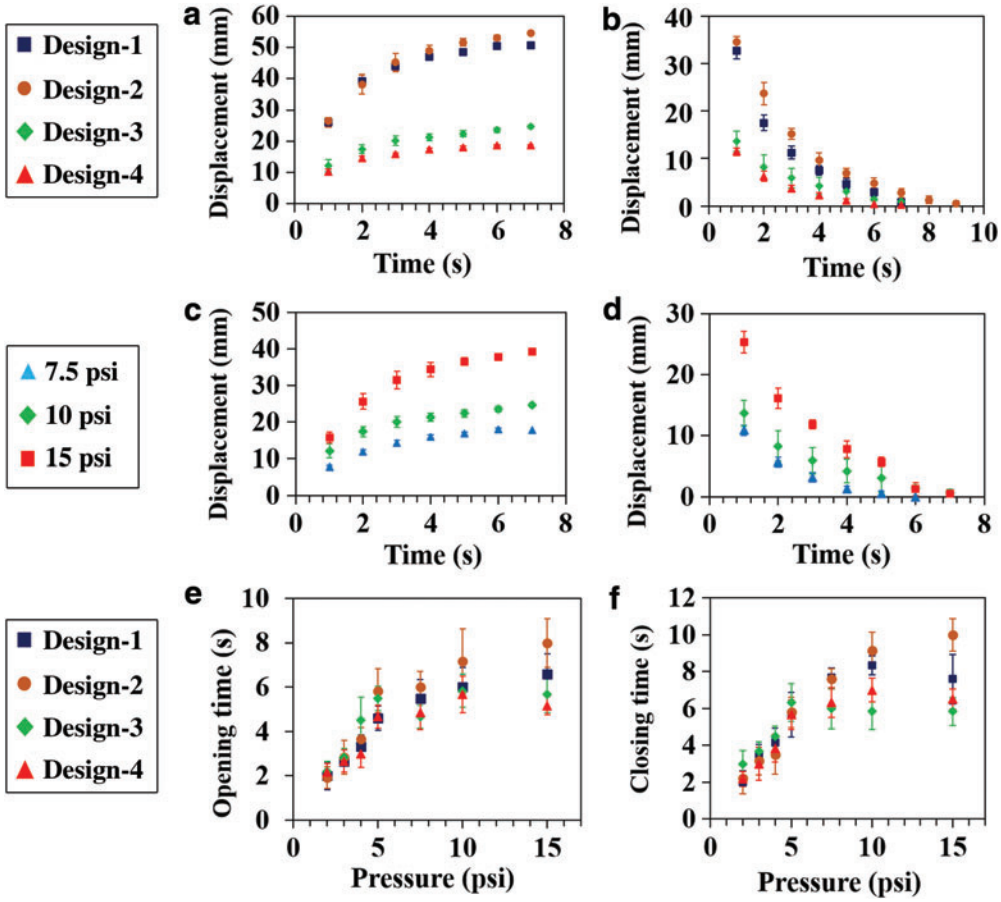

FIG. 3. Experimental characterization of flowers. **(a)** Leaf opening for all designs as demonstrated by the displacement of the leaves over time at a 10 psi air pressure set point; $t = 0$ corresponds to the time at which the valve is opened. **(b)** Leaf closing for all designs as demonstrated by the displacement of the leaves over time at a 10 psi air pressure set point; $t = 0$ corresponds to the time at which the valve is closed and air is released. **(c)** Opening of the leaves of Design-3 over time with several pressure set points between 7.5 and 15 psi; $t = 0$ corresponds to the time at which the valve is opened. **(d)** Closing of the leaves of Design-3 over time with several pressure set points between 7.5 and 15 psi; $t = 0$ corresponds to the time at which the valve is closed and air is released. **(e)** Flower opening time, defined as the time it takes to reach the maximum displacement when exposed to different pressure set points between 2 and 15 psi; $t = 0$ corresponds to the time at which the valve is opened. **(f)** Flower closing time, defined as the time is takes to reach approximately zero displacement when the pressure is at different levels (between 2 and 15 psi) at $t = 0$; $t = 0$ corresponds to the time at which the valve is closed and air is released. The error bars in all plots indicate the standard deviation over at least six trials. Color images available online at www.liebertpub.com/3dp

maximum displacement values compared with *Design-1* due to these design modifications, such as the lack of the inner leaf intended to add additional pressure to the outer leaf. Although these modifications reduce the maximum displacement of the leaves, these changes reduce the risk of breaking during use.

Characterization of opening and closing time

The displacement of the leaves over time during the opening and closing is shown in Figure 3a and b for each of the four designs tested and in Figure 3c and d for three different air pressure set points for *Design-3*. It should be noted that the air pressure in the leaves increases slowly once the valve is opened and decreases slowly after it is closed, causing the gradual opening and closing motion observed. A rapid change in displacement is observed immediately after opening or closing the valve, followed by a ''leveling off'' as the minimum or maximum displacement is reached. Based on the time-dependent opening and closing shown in Figure 3a and b for all designs, ~60% of the opening and closing displacements were observed within approximately the first 33% of the opening and closing times. Although this trend is consistent across all designs fabricated, thicker designs may experience a less dramatic ''leveling off'' of displacement. Figure 3a demonstrates that *Design-1* and *Design-2* have the greatest initial and final displacements compared with *Design-3* and *Design-4*. However, all designs reached their greatest displacement, or open position, within 8 s.

Figure 3c and d illustrate the displacement as a function of time for set point air pressures of 7.5, 10, and 15 psi. The graphs in Figure 3c and d display nonlinear behavior, and there is a difference in the curvature at 15 psi versus 7.5 psi. Thus, the same principle that governs the opening of an object attached to a hinge may apply here; a smaller pressure has a slow, steady rate, whereas a higher pressure produces rapid displacement changes that later plateau. Similarly, the greater the air pressure is when the valve is closed, the faster the initial rate of closure is, likely due to the pressure difference between the leaves and the atmosphere where a greater pressure difference causes a greater air flow rate out of the leaves. Again, 60% of the closing displacement occurs within 33% of the time; this observed behavior is consistent for all the pressure values, regardless of design. Because the behavior of *Designs-1*, *2*, and *4* mimics the behavior of *Design-3* in Figure 3a–d, the other fabricated designs are also expected to show the same pattern for change in displacement over time.

Figure 3e and f demonstrate the effect of the pressure set point on the opening and closing times, which were determined by analyzing recorded videos. In general, greater pressures result in a longer opening or closing time due to the time-dependent increase and decrease in pressure followed by opening and closing of the valve, respectively. For each given pressure, the trend in opening and closing times for each design reflects the trends observed for total displacement; this pattern implies that the time to fully open or close is directly correlated with maximum

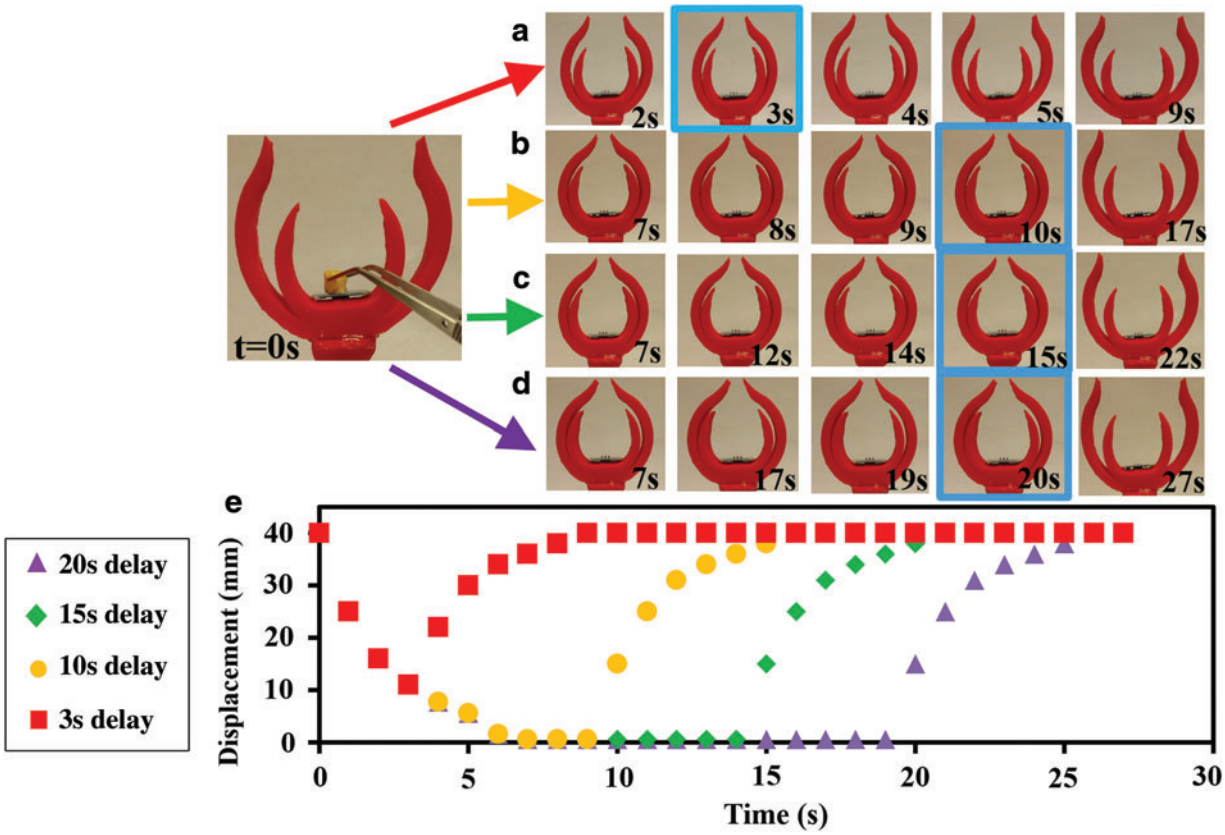

FIG. 4. Quantification of the capacitive touch sensor in terms of delay time. Time lapses of the flower in Design-3 closing and opening for **(a)** 3 s delay, **(b)** 10 s delay, **(c)** 15 s delay, and **(d)** 10 s delay. Delay time is defined as the time at which the touch sensor in Design-3 was triggered with a piece of apple to the time that the pneumatic system opens. In the 3 s delay, the leaves begin to open without fully closing; whereas in the three delays greater than 8 s, the flowers close completely. **(e)** Displacement of the leaves in Design-3 as a function of time for four different delay times. Color images available online at www.liebertpub.com/3dp

displacement experienced by each design. The design that took the longest to open, *Design-2*, also took the longest to close; similarly, *Design-3* and *Design-4* opened and closed the fastest. All designs opened within 10 s and closed within 8 s.

Characterization of the touch sensor

Results show that the plant closing is a time-dependent mechanism, requiring up to 8 s depending on the initial air pressure and the design. Therefore, to allow the flower to close completely before opening again, a delay was implemented in the system. The delay is defined as the programmed time lapse between initiation of the closing (when the touch sensor is activated and the valve is closed) and the initiation of the opening mechanism (when the valve is opened). Four different periods of delay were characterized: 3, 10, 15, and 20 s. Results showing the opening and closing mechanisms with different delays implemented are shown in Figure 4a–d, and displacements are demonstrated as a function of time for different delay times as shown in Figure 4e. At time 0, the touch sensor is triggered to initiate flower closing. The delay is seen in the frames before the frame outlined in blue. At the blue frame (occurring after the completion of the delay time, relative to time 0), the opening mechanism is triggered and all following frames show the opening of the flower. With a 3-s delay, the flower opening began before the flower had closed completely, indicating that the time delay should be set to exceed the closing time reported in Figure 3 (8 s) to allow the flower to close completely before reopening. The delay can be adjusted to control the amount of time the flower remains closed: A delay of 10, 15, and 20 s caused the flower to remain closed for $\sim$2, 7, and 12 s, respectively, after the flower completely closed at time $t = 8$.

Finite element modeling of flower

Figure 5 shows the finite element analysis (FEA) modeling of the flower for all four design conditions under four different pressures (FEA was performed in Abaqus). For each design, pressures of 0, 5, 10, and 15 psi were tested as seen in Figure 5. Under a pressure of 5 psi, the outer and inner leaves of the flower start to open and the inner surfaces of the leaves have little strain for all designs. At 10 psi, both the inner and outer leaves of *Design-1* and *Design-2* continue to open. At 15 psi, Design-1 and *Design-2* have more elastic deformation than other designs because of their geometric shape, which is consistent with the experimental results. The inner supports in *Design-3* prevent the swelling of leaves under high pressure. The simulation results of *Design-4* in Figure 5d are also consistent with the experimental result. The displacement of *Design-4* is lower than the displacement of other designs as shown in Figure 3a. The FEA shows that the simulation of designs under different pressures matches the same trend seen in the experimental results characterizing the flower designs, especially for *Design-3* and *Design-4*. However, there is one notable difference between the FEA model and the experimental results: The inner leaves in *Design-1* and *Design-2*

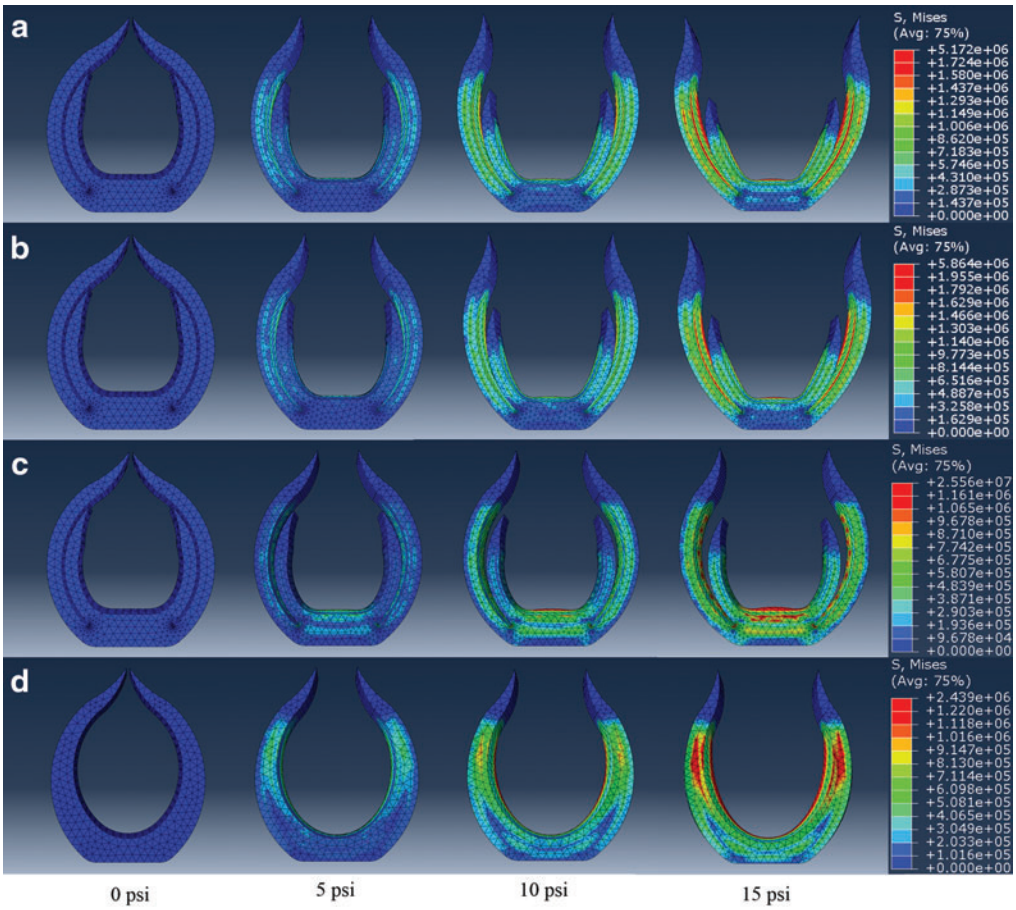

FIG. 5. FEA of Von-Mises stress in flower designs. **(a)** Results of FEA modeling of Design-1, **(b)** Design-2, **(c)** Design-3, and **(d)** Design-4 under four different pressures. FEA, finite element analysis. Color images available online at www.liebertpub.com/3dp

show displacement in the model, but they are stationary in the printed design experiments. This may be due to the inability of the printer to fabricate small channel features, preventing the smaller inner leaves from being displaced.

Conclusion

Here, a nature-inspired model of a carnivorous plant, the Venus flytrap, is developed and manufactured by using a stereolithography-based 3D printer with a flexible resin material. A touch sensor is fixed to the flowers of the plant and communicates to a pneumatic controller by sensing foreign objects in direct proximity. Once the touch sensor detects the object, it sends a signal to shut off the valve, resulting in snapping of the leaves together to ''grab'' an object. This action has been characterized by displacement as well as opening and closing time under varying air pressures. The displacement of the leaves increases when the applied pressure increases. The overall opening time and closing time are nearly equal at the same pressure force.

This study shows one avenue by which 3D printing technology will greatly assist with engineering devices such as medical prosthetics. The rapid prototyping capabilities greatly accelerated the iterative design process associated with optimizing this device. In 3D printing, one concern is often the availability of printable materials, as the material must fulfill a specific set of requirements to be compatible with 3D printing approaches. Considering the stereolithography printer used here, the material must be (i) liquid in its original state with low viscosity, (ii) photoactive under UV light to polymerize into a solid material, and (iii) flexible yet mechanically sturdy in its solid form. The printable resin used here satisfied these constraints; other printable materials are also commercially available to be compatible with both stereolithography 3D printers and fused deposition modeling and inkjet 3D printers.

The study also shows the potential of soft robotics to assist people with motor disabilities. Unlike traditional rigid robotics, the soft robotic approach implemented here can grasp delicate objects without damaging them. Thus, this approach can lead to the development of robotic devices that assist physically handicapped people to perform tasks such as grasping or lifting independently.[20]

Acknowledgments

The authors would like to thank Lorena Chanes, Anthony Guo, Christine Swol and the rest of the Fall 2015 3D Printing Class members for their enthusiastic and encouraging contribution to the final projects. S.T. acknowledges the UConn Provost's Teaching Innovation Mini Grant award, the American Heart Association Scientist Development Grant (15SDG25080056), and the University of Connecticut Research Excellence Program award for financial support of this research. S.K. acknowledges that this material is based upon work supported by the National Science Foundation Graduate Research Fellowship (DGE-1247393). We acknowledge Chu for his artful contribution to Figure 1.

Author Disclosure Statement

No competing financial interest exist.

References

1. Newsroom Archive. Nearly 1 in 5 people have a disability in the U.S., census bureau reports. www.census.gov/newsroom/releases/archives/miscellaneous/cb12-134.html, 2012. (Accessed July 10, 2016).
2. Wang Z, Chen MZQ, Yi J. Soft robotics for engineers. HKIE Trans 2015;22:88–97.
3. Shepherd RF, *et al.* Multigait soft robot. Proc Natl Acad Sci U S A 2011;108:20400–20403.
4. Kim S, Cecilia L, Trimmer B. Soft robotics: a bioinspired evolution in robotics. Trends Biotechnol 2013;31:287–294.
5. Cianchetti M, Calisti M, Margheri L, Kuba M, Laschi C. Bioinspired locomotion and grasping in water: the soft eight-arm OCTOPUS robot. Bioinspir Biomim 2015;10:035003.
6. Tricinci O, *et al.* 3D micropatterned surface inspired by salvinia molesta via direct laser lithography. ACS Appl Mater Interfaces 2015;7:25560–25567.
7. Mazzolai B. Plant-inspired growing robots. In: Soft Robotics: Trends, Applications and Challenges. Springer, 2016; pp. 57–63.
8. Amin R, *et al.* 3D-printed microfluidic devices. *Biofabrication* 2016;8:022001.
9. Knowlton S, Onal S, Yu CH, Zhao JJ, Tasoglu S. Bioprinting for cancer research. Trends Biotechnol 2015;33:504–513.
10. Knowlton S, *et al.* 3D-printed microfluidic chips with patterned, cell-laden hydrogel constructs. Biofabrication 2016; 8:025019.
11. Yenilmez B, Knowlton S, Yu CH, Heeney MM, Tasoglu S. Label-free sickle cell disease diagnosis using a low-cost, handheld platform. Adv Mater Tech 2016; 1:1600100.
12. Yenilmez B, Knowlton S, Tasoglu S. Self-contained handheld magnetic platform for point of care cytometry in biological samples. Adv Mater Tech 2016; DOI: 10.1002/admt.201600144.
13. Knowlton S, *et al.* Sickle cell detection using a smartphone. Sci Rep 2015;5:15022.
14. Knowlton S, Yu CH, Jain N, Ghiran IC, Tasoglu S. Smart-Phone based magnetic levitation for measuring densities. PloS One 2015;10:e0134400.
15. Suaste-Gomez E, Rodriguez-Roldan G, Reyes-Cruz H, Teran-Jimenez O. Developing an ear prosthesis fabricated in polyvinylidene fluoride by a 3D printer with sensory intrinsic properties of pressure and temperature. Sensors (Basel) 16:pii:E332.
16. Shi L, Guo S, Kudo H, Asaka K. Development of a venus flytrap-inspired robotic flytrap. In: Robotics and Biomimetics (ROBIO). December 11–14, 2012. Guangzhou: IEEE International Conference, 2012; pp. 551–556.
17. Grassly NC, Fraser C, Garnett GP. Host immunity and synchronized epidemics of syphilis across the United States. Nature 2005;433:417–421.
18. Pandolfi C, *et al.* Gravity affects the closure of the traps in *Dionaea muscipula.* Biomed Res Int 2014;2014:964203.
19. Hu R. Blossom' is blowing up: the story behind the 'world's first inflatable 3D print, www.core77.com/posts/26354/richard-clarksons-awesome-blossom-is-blowing-up-the-story-behind-the-worlds-first-inflatable-3d-print-26354, 2014. (Accessed July 10, 2016).
20. Polygerinos P, Galloway KC, Sanan S, Herman M, Walsh CJ. EMG controlled soft robotic glove for assistance during activities of daily living. In: 2015 IEEE International Conference on Rehabilitation Robotics (ICORR). Singapore, August 11, 2015; pp. 55–60.

Address correspondence to:
Savas Tasoglu
Department of Mechanical Engineering
University of Connecticut
Storrs, CT 06269
E-mail: savas.tasoglu@uconn.edu